

A Performance Comparison of DFIG using Power Transfer Matrix and Direct Power Control Techniques

K. Viswanadha S Murthy, M. Kirankumar, G.R.K. Murthy

Department of Electrical and Electronics Engineering, KL University, Andhra Pradesh, India

Article Info

Article history:

Received Mar 13, 2014

Revised Jun 5, 2014

Accepted Jul 2, 2014

Keyword:

Doubly-fed Induction generator (DFIG)
Direct Power control (DPC)
Power Transfer Matrix
Pulse width modulation (PWM)
Wind energy

ABSTRACT

This paper presents a direct power control and power transfer matrix model for a doubly-fed induction generator (DFIG) wind energy system (WES). Control of DFIG wind turbine system is traditionally based on either stator-flux-oriented or stator-voltage-oriented vector control. The performance of Direct Power Control (DPC) and Power transfer Matrix control for the same wind speed are studied. The Power transfer matrix Control gave better results. The validity and performance of the proposed modelling and control approaches are investigated using a study system consisting of a grid connected DFIG WES. The performance of DFIG with Power Transfer Matrix and Direct Power Control (DPC) techniques are obtained through simulation. The time domain simulation of the study system using MATLAB Simulink is carried out. The results obtained in the two cases are compared.

Copyright © 2014 Institute of Advanced Engineering and Science.
All rights reserved.

Corresponding Author:

G.R.K. Murthy,
Departement of Electrical and Electronics Engineering
KL University
Greenfields, Vaddeswaram, Guntur District, Andhra Pradesh 522502, India
Email: drgrkmurthy@kluniversity.in

1. INTRODUCTION

Generation of electricity has been largely dominated by nuclear, hydro and fossil-fueled thermal plants. Generally this type of generation is considered as conventional power generation. The main drawback of most conventional power plants is the adverse impact on the environment. The gradual depletion of fossil-fuel (such as coal, gas) reserves is also a concern. The solution to these problems lies in adopting non-conventional methods such as wind, solar etc. in power generation. Wind is regarded as the best suitable renewable energy resource for production of power and the best alternative to the conventional energy resources mainly because of availability of large wind turbines [1].

For the last two decades, research is being carried out specifically on Wind Energy Systems to capture more power at fluctuating wind speeds. With the improvement in the power electronic technology constant speed constant frequency (CSCF) generators were replaced by variable speed constant frequency (VSCF) generators in WES. The Doubly Fed Induction Generator (DFIG) is currently the choice of generator for multi-MW wind turbines. The aerodynamic system must be capable of operating over a wide wind speed range in order to achieve optimum aerodynamic efficiency by tracking the optimum tip-speed ratio. Therefore, the generator's rotor must be able to operate at a variable rotational speed. The DFIG system, therefore operates in both sub-synchronous and super-synchronous modes with a rotor speed range around the synchronous speed. The stator circuit is directly connected to the grid while the rotor winding is connected via slip-rings to a three-phase converter. For variable-speed systems where the speed range requirements are small, (for example $\pm 30\%$ of synchronous speed) the DFIG offers adequate performance and is sufficient for the speed range required to exploit typical wind resources.

The doubly fed induction generator (DFIG) based wind turbine with variable speed and variable pitch control scheme is the most popular wind power generation system in the wind power industry. This

machine can be operated either in grid connected mode or in standalone mode. This system has recently become very popular as generator for variable speed wind turbines. The major advantage of the doubly fed induction generator (DFIG), which has made it popular, is that the power electronic equipment has to handle only a fraction (20-30%) of the total system power [2], [3]. That means the losses in the power electronic equipment can be reduced in comparison to power electronic equipment that has to handle the total system power as for a direct-driven synchronous generator, apart from the cost saving of using smaller converters. Control of the DFIG is more complicated than the control of a standard induction machine. In order to control the DFIG rotor current is controlled by a power electronic converter. One common way of controlling the rotor current is by means of Field oriented (vector) control. Direct torque control (DTC) of induction machines, provides an alternative to vector control [5]. Based on the principles of DTC strategy, direct power control (DPC) was developed for three-phase pulse width modulation (PWM) converters.

Power transfer matrix is a control technique of DFIG which uses instantaneous real and reactive power instead of dq components of currents in a vector control scheme. The main features of the proposed model compared to conventional models in the dq frame of reference are [6].

a) Robustness: The waveforms of power components are independent of a reference frame; therefore, this approach is inherently robust against unaccounted dynamics such as PLL.

b) Simplicity of realization: The power components (state variables of a feedback control loop) can be directly obtained from phase voltage/current quantities, which simplify the Implementation of the control system.

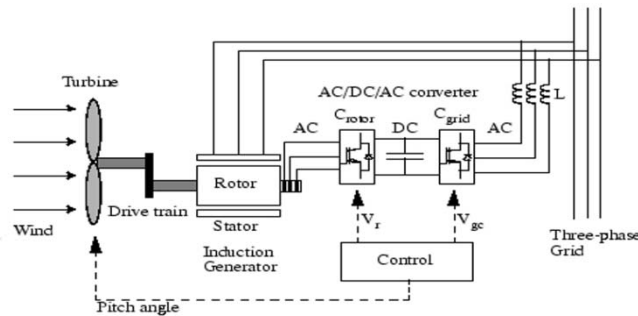


Figure 1. Structure of DFIG wind power generating system

2. WIND TURBINE MODEL

The wind turbine characteristics must be analyzed for getting optimum power curve (P_{opt}). The power output of Wind turbine is given by [4]:

$$P_0 = C_p * P_V = 0.5 \rho S_w V^3 C_p \quad (1)$$

Where ' ρ ' is the air density; S_w is wind turbine blade swept area in the wind, V is wind speed. C_p represents the power conversion efficiency of the wind turbine. It is a function of λ (Tip-speed Ratio).

$$\lambda = \frac{2\pi RN}{V_\infty} = \frac{R}{V} \omega \quad (2)$$

Where ' R ' is the blade radius; ω is the angular velocity of the rotating blades; N is the rotational speed in revolutions per second, and V_∞ is the wind speed without the interruption of rotor. C_p can be calculated by using the formula:

$$C_p = 0.5716 * \left(\frac{1}{\lambda i}\right) (116 * -0.4\beta - 5) * e^{-21 \left(\frac{1}{\lambda i}\right)} + 0.068 * \lambda \quad (3)$$

$$\frac{1}{\lambda i} = \frac{1}{\lambda + 0.08\beta} - \frac{0.035}{\beta^3 + 1}$$

Maximum power from the wind turbine is:

$$P_{max} = K \omega^3 \quad (4)$$

Where $k = 0.5S_w \left(\frac{\lambda_{opt}}{R}\right)^3 * C_p$

3. DIRECT POWER CONTROL OF DFIG

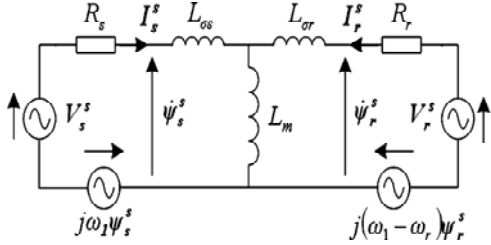


Figure 2. Equivalent circuit of DFIG in the synchronous d-q reference frame

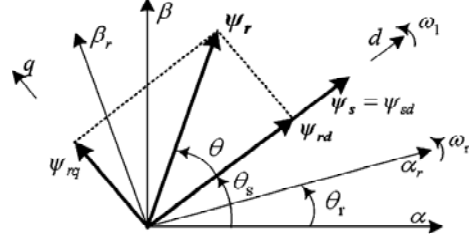


Figure 3. Stator and rotor flux vectors in synchronous d-q frame

The equivalent circuit of a DFIG in the synchronous $d-q$ frame, rotating at the speed of ω_1 , is shown in Figure 2. The d -axis of the synchronous frame is fixed to the stator flux, as shown in Figure 3. With reference to Figure 2, the stator voltage vector in the synchronous $d-q$ reference frame is given as:

$$V_s^s = R_s I_s^s + (d\Psi_s^s/dt) + j\omega_1 \Psi_s^s \tag{5}$$

Under balanced ac voltage supply, the amplitude and rotating speed of the stator flux are constant. Therefore, in the synchronous $d-q$ frame, the stator flux maintains a constant value [5]. Thus;

$$\begin{aligned} \Psi_s^s &= \Psi_{sd} \\ (d\Psi_s^s/dt) &= 0 \end{aligned} \tag{6}$$

Considering Equation (5) and neglecting the voltage drop across the stator resistance, Equation (6) can be simplified as:

$$V_s^s = j\omega_1 \Psi_s^s = j\omega_1 \Psi_{sd} \tag{7}$$

The stator current in the synchronous d-q frame is given as:

$$I_s^s = \frac{L_r \Psi_s^s - L_m \Psi_r^s}{L_s L_r - L_m^2} = \frac{\Psi_s^s}{\sigma L_s} - \frac{L_m \Psi_r^s}{\sigma L_s L_r} \tag{8}$$

Thus the stator active and reactive power inputs can be calculated as:

$$\begin{aligned} P_s - jQ_s &= 3/2 j\omega_1 \Psi_{sd} \times \left(\Psi_s^s / \sigma L_s - L_m \Psi_r^s / \sigma L_s L_r \right) \\ P_s - jQ_s &= 3/2 j\omega_1 \Psi_{sd} \times \left(\Psi_{sd} / \sigma L_s - L_m (\Psi_{rd} - j\Psi_{rq}) / \sigma L_s L_r \right) \\ P_s - jQ_s &= k\sigma\omega_1 \left[-\Psi_{sd} \Psi_{rq} + j\Psi_{sd} \left(L_r \Psi_{sd} / L_m - \Psi_{rd} \right) \right] \end{aligned} \tag{9}$$

Splitting Equation (9) into real and imaginary parts yields:

$$\begin{aligned} P_s &= -k\sigma\omega_1 \Psi_{sd} \Psi_{rq} \\ Q_s &= k\sigma\omega_1 \Psi_{sd} \left(\Psi_{rd} - \frac{L_r}{L_m} \Psi_{sd} \right) \end{aligned} \tag{10}$$

As the stator flux is constant, according to Equation (10), the active and reactive power changes over a constant period are given by :

$$\begin{aligned}\Delta P_s &= -K_\sigma \omega_1 \psi_{sd} \Delta \psi_{rq} \\ \Delta Q_s &= K_\sigma \omega_1 \psi_{sd} \Delta \psi_{rd}\end{aligned}\quad (11)$$

Equation (10) indicates that the stator reactive and active power changes are determined by the changes of the rotor flux components on the d-q axis, i.e. , $\Delta \psi_{rd}$ and $\Delta \psi_{rq}$, respectively.

4. ACTIVE AND REACTIVE POWER CONTROL

The active and reactive power control calculates the required rotor voltage that will reduce the active and reactive power errors to zero during a constant sampling time period of T_s . A PWM modulator is then used to generate the applied rotor voltage for the time period of T_s .

Within the time period of T_s , the rotor voltage required to eliminate the power errors in d-q reference frame are calculated as [7]-[9]:

$$\begin{aligned}V_{rd} &= \frac{1}{T_s} \frac{\Delta Q_s}{k_\sigma \omega_1 \psi_{sd}} - \omega_s \psi_{rq} \\ V_{rq} &= \frac{1}{T_s} \frac{-\Delta P_s}{k_\sigma \omega_1 \psi_{sd}} + \omega_s \psi_{rd}\end{aligned}\quad (12)$$

However, its accuracy could be affected by the variation of L_m (Mutual inductance). An alternative method based on Equation (11) gives:

$$\begin{aligned}\psi_{rd} &= \frac{Q_s}{k_\sigma \omega_1 \psi_{sd}} + \frac{L_r}{L_m} \psi_{sd} \\ \psi_{rq} &= \frac{-P_s}{k_\sigma \omega_1 \psi_{sd}}\end{aligned}\quad (13)$$

From the Equation (12) and (13) we get:

$$\begin{aligned}V_{rd} &= \frac{1}{T_s} \frac{\Delta Q_s}{k_\sigma \omega_1 \psi_{sd}} + \omega_s \frac{P_s}{k_\sigma \omega_1 \psi_{sd}} \\ V_{rq} &= \frac{1}{T_s} \frac{-\Delta P_s}{k_\sigma \omega_1 \psi_{sd}} + \omega_s \left(\frac{Q_s}{k_\sigma \omega_1 \psi_{sd}} + \frac{L_r}{L_m} \psi_{sd} \right)\end{aligned}\quad (14)$$

The first terms on the right hand side reduce power errors while the second terms compensate the rotor slip that causes the different rotating speeds of the stator and rotor flux.

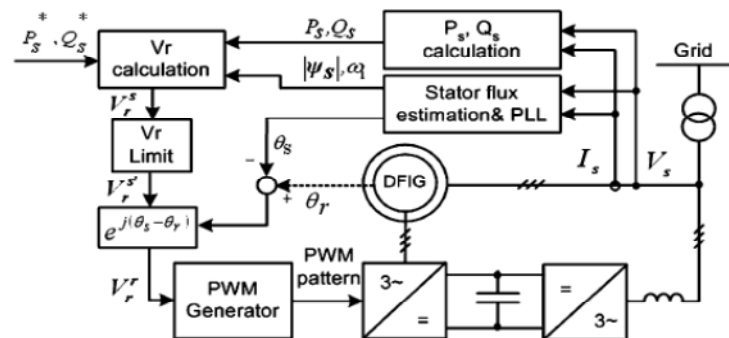


Figure 4. Schematic diagram of the DPC for a DFIG system

5. PRINCIPLES OF POWER TRANSFERMATRIX

The schematic diagram of a DFIG wind turbine generator is represented in Figure 1. The power Converter includes Rotor-side-converter (RSC) to control speed of the generator and Grid-side converter (GSC) to inject reactive power to the system. The instantaneous real and reactive power components of the grid side converter, $p_g(t)$ and $q_g(t)$ in the synchronous d-q frame of reference are [6]:

$$\begin{bmatrix} p_g(t) \\ q_g(t) \end{bmatrix} = \frac{3}{2} \begin{bmatrix} v_{sd} & v_{sq} \\ v_{sq} & -v_{sd} \end{bmatrix} \begin{bmatrix} i_{gd} \\ i_{gq} \end{bmatrix} \quad (15)$$

6. MODEL OF DFIG USING INSTANTANEOUS POWER COMPONENTS

The change in real power and reactive power can be expressed as [12]-[14]:

$$\begin{aligned} \frac{dp_s}{dt} &= g_1 p_s - \omega_{sl} q_s - g_4 \psi_{sd} - g_5 \psi_{sq} + u_{rd} \\ \frac{dq_s}{dt} &= \omega_{sl} p_s + g_1 q_s + g_4 \psi_{sq} - g_5 \psi_{sd} + u_{rd} \end{aligned} \quad (16)$$

Where,

$$\begin{aligned} u_{rd} &= g_2 v_{rd} + g_3 v_{rq} - 3 \frac{v_s^2}{2L_s} \\ u_{rq} &= g_3 v_{rd} - g_2 v_{rq} \\ g_1 &= -\frac{r_s L_r + L_s r_s}{L_s L_r}; g_2 = \frac{3L_m v_{sd}}{2L_s L_r} \\ g_3 &= \frac{3L_m v_{sq}}{2L_s L_r} \\ g_4 &= \frac{3}{2} \left(\frac{r_r v_{sd} - L_r \omega_r v_{sq}}{L_s L_r} \right) \\ g_5 &= \frac{3}{2} \left(\frac{r_r v_{sd} + L_r \omega_r v_{sq}}{L_s L_r} \right) \end{aligned} \quad (17)$$

The electromechanical dynamic model of the machine is:

$$\frac{d\omega_r}{dt} = \frac{P}{J} (T_e - T_m) \quad (18)$$

Where P, J and T_m are the number of pole pairs, inertia of the rotor, and mechanical torque of the machine, respectively. The electric torque is given by [10], [11]:

$$T_e = \frac{3}{2} P (\psi_{sd} i_{sq} - \psi_{sq} i_{sd}) \quad (19)$$

$$\frac{d\omega_r}{dt} = g_6 p_s + g_7 q_s - \frac{P}{J} T_m \quad (20)$$

Where,

$$\begin{aligned} g_6 &= \frac{P^2}{J} \frac{\psi_{sq} v_{sd} - \psi_{sd} v_{sq}}{v_s^2} \\ g_7 &= \frac{P^2}{J} \frac{\psi_{sd} v_{sd} + \psi_{sq} v_{sq}}{v_s^2} \end{aligned} \quad (21)$$

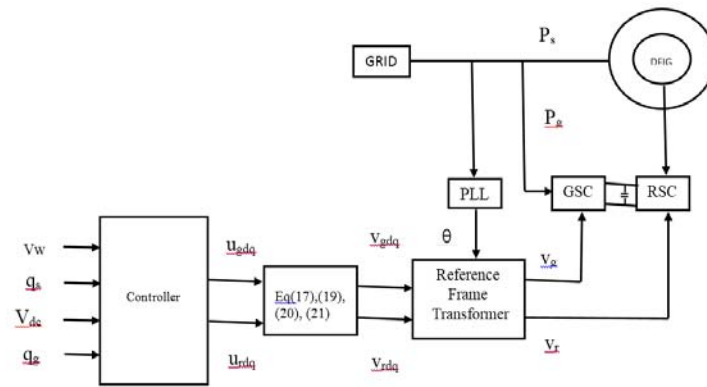


Figure 6. Schematic diagram of the study system of power transfer matrix

6. RESULTS AND COMPARISON

The following parameters are used to verify the real power, Reactive power and dc link voltages:

Parameters	Values	Units
Rated power(P)	1.5	MW
Rated voltage(V)	0.575	KV
Rated frequency(F)	60	Hz
Rated wind speed(V _w)	12	m/s
Stator resistance(R _s)	1.4	mΩ
Rotor resistance(R _r)	0.99	mΩ
Stator leakage inductance(L _s)	89.98	μH
Rotor leakage inductance(L _R)	82.08	μH
Magnetization inductance(L _m)	1.526	mH
Stator/rotor turns ratio	1	-
Poles	6	-
Turbine rotor diameter	70	M
Lumped inertia constant	5.05	S

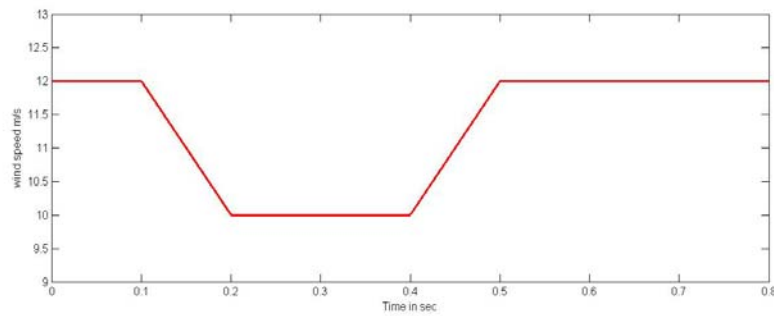


Figure 7. Trapezoidal pattern for wind speed

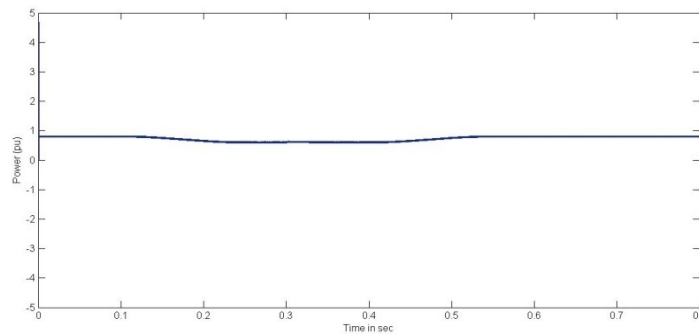


Figure 8(a). Real power from power transfer matrix control

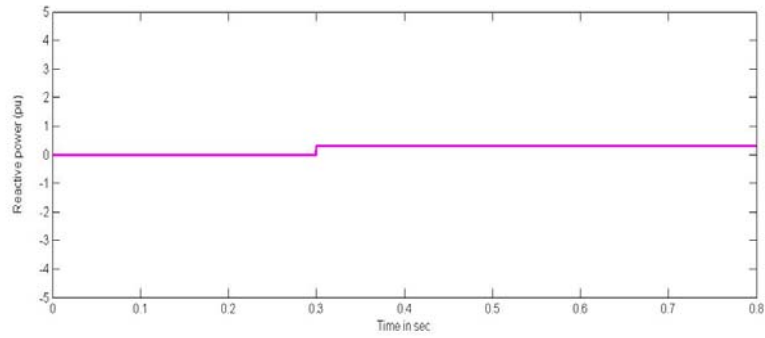


Figure 8(b). Reactive power from power transfer matrix control

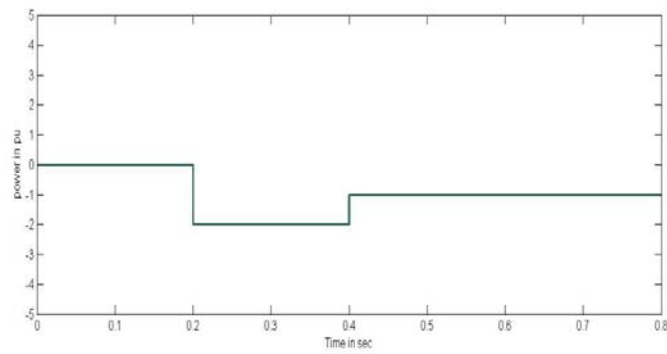


Figure 9(a). Real power from DPC

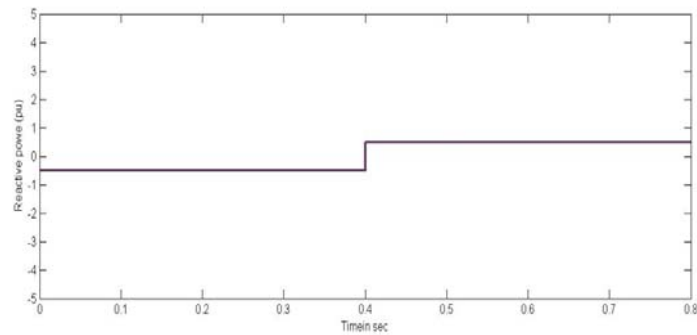


Figure 9(b). Reactive power from DPC

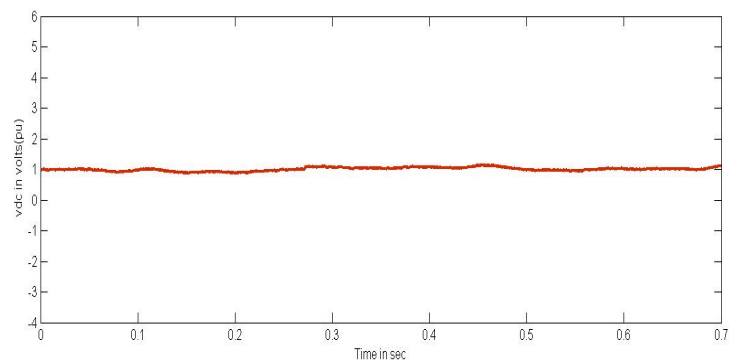


Figure 10(a). Vdc from Power transfer matrix

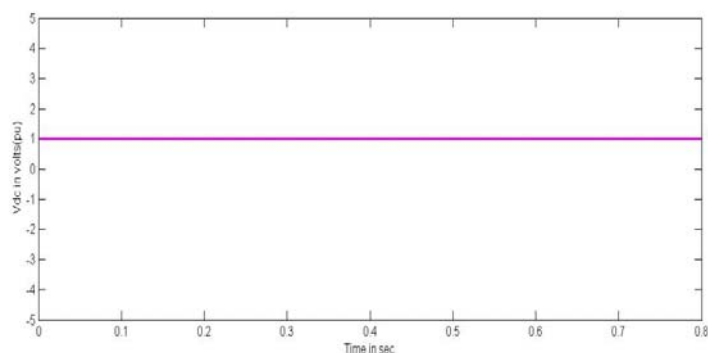


Figure 10(b). Vdc from DPC

The results are obtained at a wind speed of 12 m/sec. The trapezoidal wave form shown in Figure 7 shows the pattern of step change in the reactive reference which is applied to both the control techniques. The trapezoidal pattern was selected to examine the system behavior following variation in the wind speed with both negative and positive slopes. The selected wind speed pattern spans an input mechanical wind power from 0.7 to 1 p.u. (70 to 100% of the turbine-generator rated power).

Figures 8(a) and 8(b) show the Real and Reactive power tracking of DFIG against disturbances present in the given wind speed pattern. Because of coupling of all powers interlinked to each other, the coupling effect is obtained at $t=0.3$ sec.

Figure 9(a) shows the Real power tracking of DFIG against disturbances in the given wind speed pattern. Here the dip in the wave form shows the start of real power generation at $t=0.2$ sec. Figure 9(b) indicates the reactive power absorption for 0.4 sec.

Figures 10(a) and 10(b) show the dc link voltages of Power transfer matrix control and DPC. The change in wind speed leads to the fluctuations of the dc link voltage. Due to the coupling of all powers v_{dc} of power transfer matrix have some variations. Whereas in DPC there is no coupling of the powers and the dc link voltage is constant. Change in wind speed does not affect dc link voltage.

7. CONCLUSION

Upon examining the results of both Power transfer matrix and DPC techniques for the same disturbances the Real power generation is better in power transfer matrix control than with DPC. Also the generation of power starts in DPC with a delay of 0.2 sec. Hence power transfer matrix method is giving better results than the DPC method.

REFERENCES

- [1] Wind technology 2011024/29. Global wind energy council (online). Available at www.gwec.net
- [2] LH Hansen, L Helle, F Balaabjerg, E Ritchie, S munk-nielsen, H binder. *Conceptual Survey of Generators And Power Electronics For Wind Turbines*. Riso national laboratory.
- [3] L Morel, H Godfroid. *Dfim Converter Optimisation And Field Oriented Control Without Positioning Sensor*. IEE proc. electr. power appl. 1998; 145(4): 360-368.
- [4] SN Bhadra, D Kastha, S Banarjee. *Wind Electrical Systems*. Oxford University press
- [5] Dawei Zhi, Lie Xu. *Direct Power Control of DFIG with Constant Switching Frequency and Improved Transient Performance* *IEEE Transactions on Energy Conversion*. 2007; 22(1).
- [6] Esmaeil Rezaei, Ahmadreza Tabesh, Mohammad Ebrahimi. Dynamic Model and Control of DFIG Wind Energy Systems Based on Power Transfer Matrix. *IEEE Transactions on Power Delivery*. 2012; 27(3).
- [7] P Krause, O Wasynczuk, S Sudhoff, IPE Society. *Analysis of Electric Machinery and Drive Systems*. Piscataway, NJ: IEEE. 2002.
- [8] Abdelmalek Boulahia. Mentouri university of Constantine, Algeria; Khalil NABTI; Hocine BENALLA, Algeria Direct Power Control for Threelevel NPC Based PWM AC/DC/AC Converter in Doubly Fed Induction Generators Based Wind Turbine International Journal of Electrical and Computer Engineering (IJECE). 2012; 2(3): 425-436.
- [9] NRN Idris, AHM Yatim. *Direct Torque Control of Induction Machines with Constant Switching Frequency and Reduced Torque Ripple*. *IEEE Trans. Ind. Electron.*, 2004; 51(4): 758-767.
- [10] J Kang, S Sul. New Direct Torque Control of Induction Motor for Minimum Torque Ripple and Constant Switching Frequency. *IEEE Trans. Ind. Appl.*, 1999; 35(5): 1076-1082.

-
- [11] T Noguchi, H Tomiki, S Kondo, I Takahashi. Direct Power Control Of Pwm Converter Without Power-Source Voltage Sensors. *IEEE Trans. Ind. Appl.*, 1998; 34(3): 473–479.
- [12] G Escobar, AM Stankovic, JM Carrasco, E Galvan, R Ortega. Analysis and Design Of Direct Power Control (Dpc) For A Three Phase Synchronousrectifier Via Output Regulation Subspaces. *IEEE Trans. Power Electron.*, 2003; 18(3): 823–830.
- [13] M Malinowski, MP Kazmierkowski, S Hansen, F Blaabjerg, GD Marques. VIRTUAL-FLUX-BASED DIRECT POWER CONTROL OF THREE-PHASEPWM RECTIFIERS. *IEEE Trans. Ind. Appl.*, 2001; 37(4): 1019–1027.
- [14] KP Gokhale, DW Karraker, SJ Heikkila. *Controller for A Woundrotor Slip Ring Induction Machine*. U.S. Patent 6 448 735 B1. 2002.
- [15] L Xu, P Cartwright. Direct active and reactive power control of DFIGfor wind energy generation. *IEEE Trans. Energy Convers.*, 2006; 21(3): 750–758.
- [16] Wang Zezhong, Liu Qihui. Analysis of DFIG Wind Turbine during Steadystate and Transient Operation. *TELKOMNIKA Indonesian Journal of Electrical Engineering*. 2014; 12(6): 4148-4156.